Journal of Materials Chemistry A

Accepted Manuscript

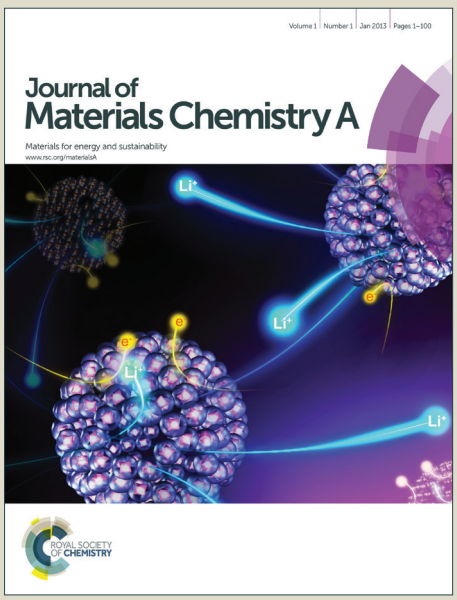

ROYAL SOCIETY OF CHEMISTRY

www.rsc.org/materialsA

Journal Name

RSCPublishing

ARTICLE

Electrochemical Supercapacitor with Polymeric Active Electrolyte

Cite this: DOI: 10.1039/x0xx00000x

Libin Chen, Yanru Chen, Jifeng Wu, Jianwei Wang, Hua Bai*, and Lei Li*

Received 00th January 2012,
Accepted 00th January 2012

DOI: 10.1039/x0xx00000x

www.rsc.org/

An electrochemical supercapacitor with polymeric active electrolyte was designed and fabricated in this paper. A water soluble conducting polymer, sulfonated polyaniline (SPAni), was used in the supercapacitor as the active electrolyte, and semipermeable membrane was employed as the separator of the device. It was found that SPAni in the electrolyte can provide pseudocapacitance via its reversible electrochemical redox reaction. Owing to the good stability of SPAni, the supercapacitor has long cycling life. Moreover, the migration of SPAni between two electrodes was blocked by the semipermeable membrane separator, thus self-discharge caused by the shuttle effect of SPAni was suppressed. The research in this paper demonstrated the possibility of using polymer as active electrolyte in supercapacitor, and paved a new way to active electrolyte enhanced supercapacitors with high capacitance and good energy retention.

Introduction

Electrochemical supercapacitors (ESCs) are storage devices for electric energy which own much higher power density compared with batteries, thus are important for those applications requiring large current supply, such as electrical vehicles.[1,2] Two basic types of ESCs are commonly described in the literatures depending on the mechanism of energy store: electrochemical double layer supercapacitors (EDLSCs), in which the energy is stored by ion adsorption on the surface of electrodes,[3–5] and pseudocapacitors, in which fast surface redox reactions are employed to store energy.[1] Pseudocapacitors usually have higher specific capacitance than EDLSCs, thus receive considerable attention in recent years.[6–8] The surface redox reactions in pseudocapacitors can be achieved by modifying electrode with electroactive materials, or using soluble redox active electrolytes. Incorporation of redox active species in electrolyte solution, compared with modification of electrode with redox materials, is much easier to carry out, and compatible with the current fabrication technology of supercapacitor. Recently, various redox active small molecules or ions, including hydroquinone (HQ),[9–12] ferricyanide ($Fe(CN)_6^{4-}$),[13,14] iodide (I^-),[15] methylene blue,[16] phenylenediamine,[17,18] have been used in supercapacitor to achieve high pseudocapacitance (active electrolyte enhanced supercapacitor, AEESC). The specific capacitance (C_s) values were greatly improved after the addition of the redox electrolytes. For example, Ricardo *et al.* successfully increased the C_s of carbon-based ESCs from ~320 F g^{-1} to 901 F g^{-1} by using redox active electrolyte HQ.[10]

Although redox electrolytes can significantly increase the C_s of ESCs, they also bring serious problem: fast self-discharge (SDC). It has been found by us and other groups that SDC process was obviously accelerated after active electrolytes were incorporated into ESCs.[15,19,20] SDC rate is the index of energy retention of an ESC, and fast SDC will strongly limit the practical application of ESC. As demonstrated in our previous report, the fast SDC of AEESC is caused by the shuttle effect of active electrolyte. The electrolysis products of the active species generated on one electrode diffuse to another electrode, where they deplete the charges stored on the electrode through inverse electrochemical reaction.[20] Therefore, in order to suppress the fast SDC of AEESC, the shuttle of active electrolyte between two electrodes must be blocked.[19,20] There can be two ways to stop the shuttle of small molecule active electrolyte between two electrodes. One strategy is to choose a special active electrolyte. As we reported, no shuttle effect was found when Cu^{2+} was used as active electrolyte, which was converted to insoluble Cu and deposited onto the electrode during charge process.[20] Therefore, there will be no migration of electrochemical product. Another strategy is to use an ion-exchange membrane as the separator of the device, which can block the migration of active electrolyte.[19] However, anion-exchange membrane separator is expensive, increasing the cost of ESCs and limiting their practical application.

Herein, we design a new type of AEESC, based on polymeric active electrolyte and volume-selectively semipermeable

separator (polymeric active electrolyte enhanced supercapacitor, PAEESC). The semipermeable membrane can block the diffusion of bulky polymeric active electrolyte, but allows free migration of small ions. Consequently, the SDC caused by shuttle effect was suppressed efficiently. A commonly-used regenerated cellulose dialysis tube with molecular weight cut-off (MWCO) of 8000 ~ 14000 was employed as the separator, and sulfonated polyaniline (SPAni) as polymeric active electrolyte. SPAni has good redox activity and stability, and is easy to synthesis and commercially available. As a result of the use of polymeric redox active electrolyte and semipermeable membrane, the C_s of the ESC device was improved without obvious degradation of energy retention.

Experiments

Materials

Concentrated sulfuric acid (98%), sodium nitrate, hydrochloric acid and hydrazine hydrate (80%) were purchased from Xilong Chemical Industry Incorporated Co. Ltd. Potassium permanganate, hydrogen peroxide (30%), aniline, ammonium persulfate, chlorosulfonic acid and hydroquinone were bought from Sinopharm Chemical Reagent Co., Ltd. SPAni was synthesized in our lab following the previous procedures (See Fig. S1 ~ S3 for the spectra data of SPAni†).[21,22] Graphene oxide (GO) was prepared from natural graphite (325 mesh, Qingdao) according to modified Hummers' method.[23,24] Dialysis tube with MWCO of 8000 ~ 14000 is the product of Viskase.

Assemble of the Supercapacitor Device

Two-electrode device configuration was used in this work, and graphene hydrogel (GHG) was chosen as the electrode. GHG was prepared by hydrothermal reduction of GO, and further treated with hydrazine, according to the method reported by Zhang *et al*. (Fig. S4†).[25] Before assemble of the device, the GHG blocks were compressed to thin discs (diameter ~ 8 mm, thickness ~ 1.5 mm). Two pieces of Pt foil（2 × 2 cm^2）were used as current collectors. To seal the device, a silicone ring was sandwiched between the Pt foils, with graphene gel, separator, and electrolyte solution accommodated in it. The electrolyte solution was 0.1 M SPAni + 4 M H_2SO_4 (Device 2). For caparison, devices with 4 M H_2SO_4 (Device 1) or 0.1 M HQ + 4 M H_2SO_4 (Device 3) as electrolyte were also assembled. To investigate the electrode process of single electrode, a three-electrode cell was used. The above two-electrode device was immersed into an electrochemical cell filled with the same electrolyte as used in the device. Two openings were cut on the silicon rubber gasket, to ensure the connectivity of the electrolyte in the device and the cell. The two electrodes of the device were used as working and counter electrode, and a saturated calomel electrode (SCE) was utilized as the reference electrode.

Measurements

The morphologies of GHG and the separator were observed on a scanning electron microscope (SEM, LEO1530) operated at 20 kV. All the electrochemical measurements were conducted in CHI 660 electrochemical workstation. A three electrode system was used to investigate the electrochemical properties of SPAni, in which glassy carbon (GC, ϕ = 3 mm) or GHG modified GC electrode was employed as working electrode, and a platinum foil (1 cm × 1 cm) and a SCE as counter and reference electrode. The ESC devices were tested by cyclic voltammetry (CV), galvanostatic charge-discharge (GCD) and AC impedance. The C_s of the device was calculated according to the following equations:

$$C_S = \frac{Jt}{V - IR}, \quad (1)$$

$$J = \frac{I}{m}, \quad (2)$$

where J is the mass current density, I is the current applied on the device, t is the discharge time, m is the total mass of two electrode, V is the highest voltage in the GCD curves, and IR represents the voltage drop at the beginning of the discharge process. The specific capacitance of single electrode was calculated from the potential curves measured with three-electrode system:

$$C_+ \text{ or } C_- = \frac{Jt}{\Delta V - IR}, \quad (3)$$

$$J = \frac{I}{m}, \quad (4)$$

where m is the mass of single electrode, and V is the potential change of the electrode during discharge process; I, t and IR have the same definitions as in Eqn. 1 and 2.

Results and discussion

Fig. 1 represents the CV and GCD curves of the ESCs with H_2SO_4 (Device 1) and SPAni-H_2SO_4 (Device 2) as electrolyte, respectively. The CV curves of Device 1 (Fig. 1A) are nearly rectangular, with a pair of weak redox waves, which are attributed to the redox reaction of oxygen-contain groups on chemically reduced graphene (CCG).[26] The current density in the CV curves is proportional to the scan rate (Fig. S5†), indicating that the electrode process is not controlled by diffusion.[27] Such a linear relationship between current density and scan rate is the characteristic of a capacitor. The GCD curves of Device 1 are shown in Fig. 1B, which have triangular shape. The C_s of Device 1 was calculated from GCD curves according to Eqn. 1. At a current density of 0.88 A g^{-1}, the C_s of Device 1 is 52.5 F g^{-1}, and it decreases slightly to 47.5 F g^{-1} when the current density rise to 4.42 A g^{-1}. These values agree well with the reported results (C_s of single electrode reported by Zhang et al. was 205 F g^{-1} at 1 A g^{-1}, corresponding to a C_s of device of 51.2 F g^{-1} at 0.5 A g^{-1}),[25] demonstrating good performance of our GHG electrodes.

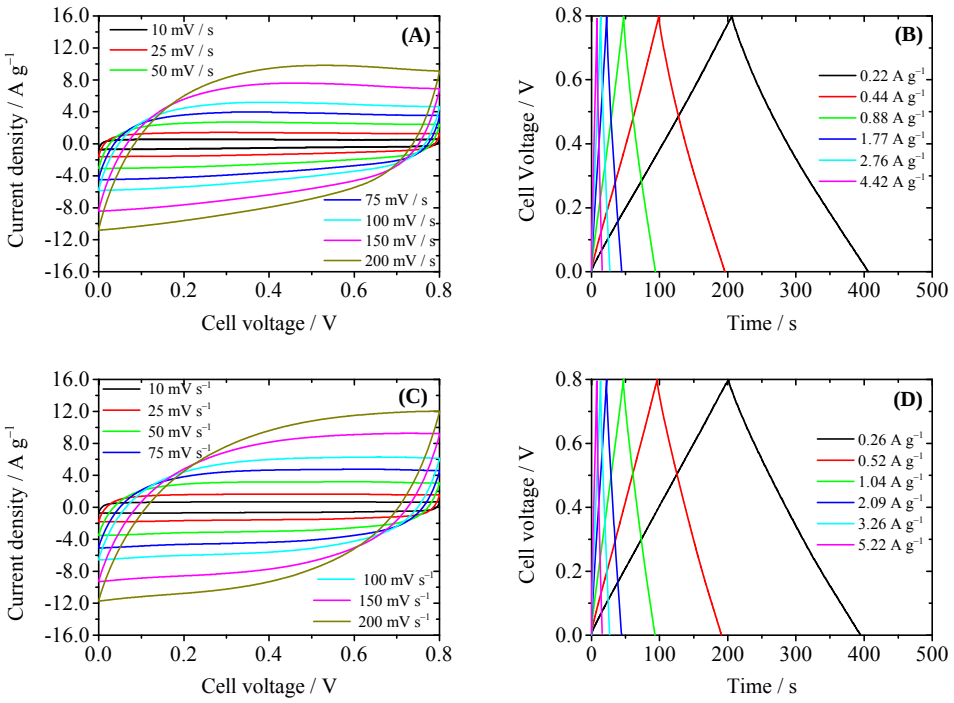

Fig. 1 Performance of Device 1 (4 M H_2SO_4) and Device 2 (0.1 M SPAni + 4 M H_2SO_4, with semipermeable membrane as separator). (A)(B) CV and GCD curves of Device 1. (C)(D) CV and GCD curves of Device 2.

The CV and GCD curves of Device 2 are shown in Fig. 1C and D. Compared with those of Device 1, the CV curves (Fig. 1C) of Device 2 have larger current density, but their shapes are still deformed rectangle. The current density in these CV curves is also proportional to the scan rate, showing the characteristic CV behavior of ideal capacitor (Fig. S6†). The GCD curves shown in Fig. 1D are nearly triangular, which correspond with the CV curves. The C_s values of Device 2 calculated from the GCD curves are represented in Fig. 2. A C_s value of 57 F g^{-1} at 5.22 A g^{-1} was obtained for Device 2, 20% higher than that of Device 1. When the current density increases from 0.26 to 5.22 A g^{-1}, the C_s value of Device 2 only decreases by 10.6%, showing good rate performance (For Device 1, when the current density increases from 0.22 to 4.42, A g^{-1}, the C_s value decreases by 14.4%). The cycling stability of the Device 2 was also studied by GCD at a constant current density of 1.04 A g^{-1}. As shown in Fig. 3, the C_s of Device 2 remains 99% after 1000 cycles. The stability of the capacitor is good enough for practical application. In fact, polyaniline and its derivatives usually have good electrochemical stability. Moreover, the electrochemical reactions of SPAni take place in the electrolyte, thus during charge/discharge cycles, there will be no obvious change in the volumes of electrodes. In many devices, the repeating volume change of electrodes, caused by electrochemical reaction of the electroactive materials in the electrodes, will damage the good electric contact between electrode and current collector, leading to degradation of the device performance.[28] Therefore, stable active materials and suitable device structure endue Device 2 with good cycle stability.

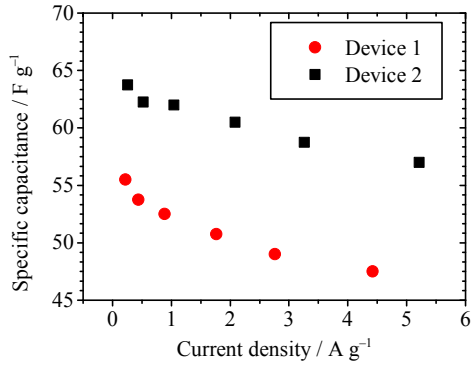

Fig. 2 Specific capacitance of Device 1 (4 M H_2SO_4) and Device 2 (0.1 M SPAni + 4 M H_2SO_4, with semipermeable membrane as separator) at different current densities.

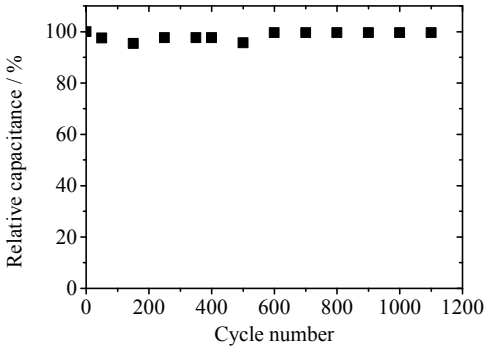

Fig. 3 Cycling stability of Device 2 (0.1 M SPAni + 4 M H_2SO_4, with semipermeable membrane as separator) upon GCD at a current density of 1.04 A g^{-1}.

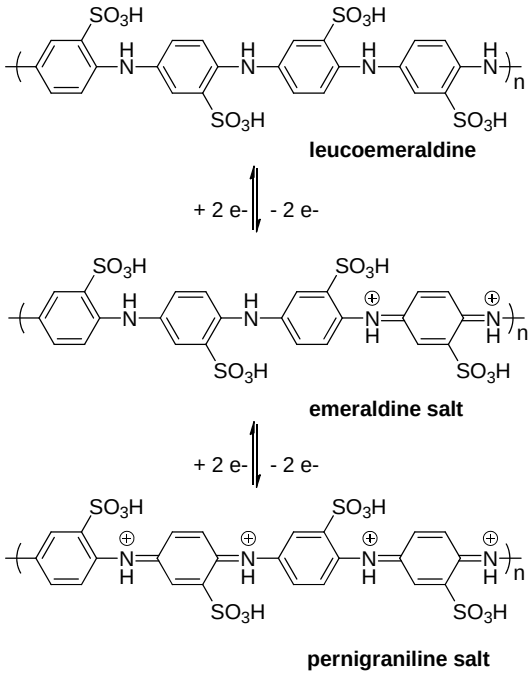

Scheme 1. Reversible redox reactions of SPAni in acidic medium.

To elucidate the working mechanism of SPAni-containing AEESC, the electrochemical properties of SPAni was investigated. Fig. 4 depicts the CV curves of GC and GHG modified GC electrodes in 4 M H_2SO_4 or 0.1 M SPAni + 4 M H_2SO_4 solution. In H_2SO_4 the CV curve of GHG modified GC electrode (Curve a) is a tilt rectangle, showing large EDL capacitance. A pair of wide redox waves at ~ 0.3 V are found in the CV curve, which are related to the residual oxygen-containing functional groups on CCG sheets. The CV curve of bare GC electrode in SPAni/H_2SO_4 solution (Curve b) shows much lower charging current, due to the smaller surface area of GC electrode. There are two pairs of redox waves in this CV curve, a small pair at 0.45 V *vs.* SCE and a large pair at 0.65 V *vs.* SCE. These waves can be attributed to the transition of polyaniline backbone between its different doping states, namely, from leucoemeraldine to emeraldine (0.45 V), and from emeraldine to pernigraniline (0.65 V), as illustrated in Scheme 1.[29,30] The CV curve of GHG in SPAni/H_2SO_4 solution (Curve c) is the superposition of Curve a and b. The oxidization peak of SPAni at 0.65 V *vs.* SCE is also found in Curve c, indicating that the electrochemical oxidation processes of SPAni on GHG and GC are identical. The peak current in Curve c is larger than that in Curve b, also due to large electrode surface area. Therefore, from the CV study it is concluded that SPAni is able to provide pseudocapacitance when the electrode potential is above 0.45 V *vs.* SCE.

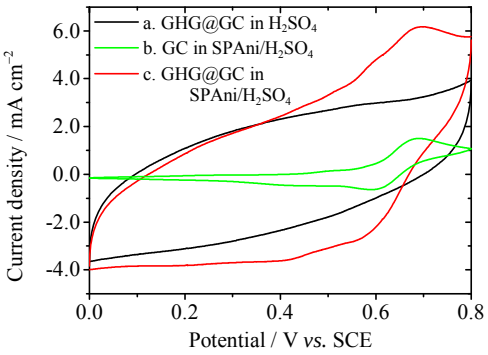

Fig. 4 CV curves of H_2SO_4 or SPAni/H_2SO_4 on different electrodes at a scan rate of 25 mV s^{-1}.

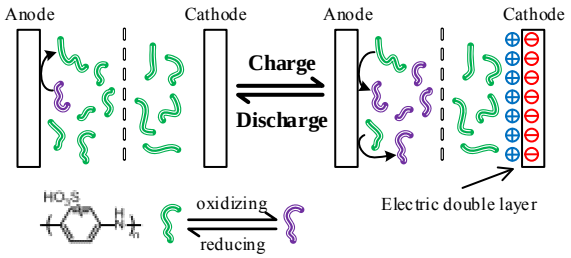

Scheme 2. Working mechanism of Device2 (0.1 M SPAni + 4 M H_2SO_4, with semipermeable membrane as separator).

The electrode process of each electrode in Device 2 during GCD was investigated in a three-electrode configuration system. In such configuration, the variation of potential of each electrode can be monitored. Fig. 5 shows evolution of the cell voltage and the potential of each electrode during GCD process. From Fig. 5 it is easy to conclude that Device 2 is an asymmetric supercapacitor. The equilibrium potential of both electrodes are ~ 0.4 V *vs.* SCE. This is determined by the equilibrium potential of the reaction from leucoemeraldine to emeraldine. When the supercapacitor is charged, the potential of the anode increases from 0.4 to 0.6 V *vs.* SCE, while that of the cathode decreases from 0.4 to −0.2 V *vs.* SCE. In the potential range of −0.2 to 0.4 V *vs.* SCE, there is no redox reaction related to SPAni, as demonstrated by the CV curves in Fig. 4, thus the capacitance of cathode is mainly EDL capacitance (Scheme 2). The small plateau in the potential curve of cathode at the potential of −0.2 V *vs.* SCE is caused by decomposition of water.[20,31] The C_s of cathode is calculated to be 190 F g^{-1}, in agreement with the literature data.[25] However, for anode, its potential changes much slower compared with that of cathode in GCD process, indicating a larger anode capacitance. The specific capacitance of anode is 361 F g^{-1} according to the potential curve in Fig. 5. Since the capacitance of the device is the series capacitance of two electrodes, it will be enhanced by the large capacitance of anode. These results are similar with the reported AEESCs based on small active molecules or ions.[9] As depicted in Scheme 2, in charge process, the anode current is consumed by SPAni molecules, which are oxidized from leucoemeraldine to emeraldine and

pernigraniline. As a result, only a small portion of the current is utilized to charge the EDL of anode, leading to small potential shift (depolarization of SPAni), and large apparent capacitance. In other word, on anode the charges are stored in SPAni molecules, rather than in EDL. In discharge process, pernigraniline undergoes a reverse reduction reaction, releases the stored charges and returns to leucoemeraldine. Therefore, in anode camber the electric energy is store in oxidized SPAni molecules in electrolyte solution, but in cathode camber is on the surface of electrode (in EDL). We also investigate the influence of SPAni concentration on the performance of the device. It was found that in the range of 0.02 M ~ 0.1 M, the concentration of SPAni has little effect on the C_s of the device (See Fig. S7). This result demonstrates that at these concentration, there are always enough SPAni on the surface of anode during charge process, even the depletion effect of SPAni caused by constant-current electrolysis is considered. It should be noted that, an asymmetric device structure, with small anode mass and large cathode mass, can further improve the specific capacitance of Device 2, by balancing the capacitances of two electrodes.

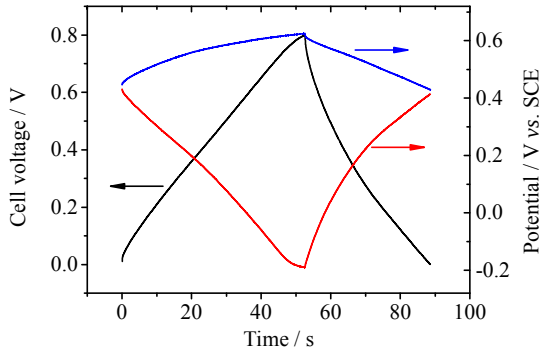

Fig. 5 Potential curves of single electrode of Device 2 (0.1 M SPAni + 4 M H_2SO_4, with semipermeable membrane as separator) during GCD. Current density: anode, 3.07 A g^{-1}; cathode, 2.71 A g^{-1}.

In charged device, if the oxidized SPAni molecules can penetrate through the separator, they will come into contact with cathode, whose potential is lower than their equilibrium potential. Thus these molecules will be reduced by cathode, causing SDC. Such SDC process is commonly found in AEESC. Therefore, in Device 2, we used size-selective semipermeable membrane (dialysis tube) as the separator, to block the shuttle of SPAni between two electrodes. In our dialysis experiment, after 48 h, no SPAni was detected by UV-Vis spectrum in the diffusate, thus the dialysis tube with MWCO of 8000~14000 can efficiently block the diffusion of SPAni. Fig. 6 compares the SDC rate of Device 1 and Device 2. Device 1 as a pure EDLSC was used as the reference, whose SDC process is considered to be govern by ion diffusion.[32,33] If the SDC rate of Device 2 is not larger than that of Device 1, it can be concluded that SPAni does not accelerate the SDC process. To demonstrate the importance of semipermeable membrane separator, the SDC curve of another device, which was identical to Device 2 except that the separator was replaced by porous cellulose acetate membrane (pore size: 220 nm, Fig. S12†), was also measured (Device 3). All the devices were charged to 0.8 V and then their open circuit voltages were recorded. As shown in Fig. 6, Device 2 and Device 1 have similar SDC rates. 10000 s later, the voltage of Device 2 is 0.38 V, only 0.01 V lower than that of Device 1. After 18000 s, the cell voltage of Device 2 even becomes large than that of Device 1. As a comparison, in 10000 s the cell voltage of Device 3 dwindles down to 0.23 V, such lower than Device 2. These results clearly demonstrated that semipermeable membrane successfully block the migration of SPAni between anode and cathode cambers, thus suppress the SDC. In another control experiment, we fabricated another device, in which the active electrolyte SPAni in Device 2 was replaced by HQ, a small molecule (Device 4). Because HQ can pass through the semipermeable membrane, the SDC rate of Device 4 is obviously larger than Device 2 (Fig. S13†). Therefore, in order to suppress fast SDC process, both the polymeric active electrolyte with large molecular mass and size-selective semipermeable membrane are necessary for this type of device.

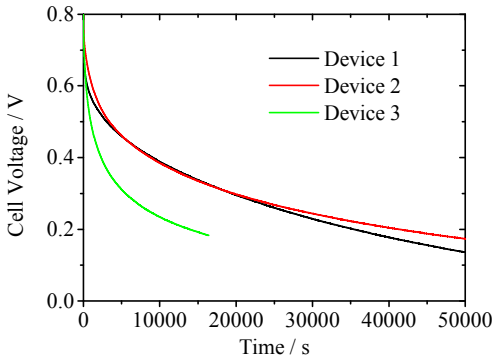

Fig. 6 Self-discharge curves of Device 1 (4 M H_2SO_4), Device 2 (0.1 M SPAni + 4 M H_2SO_4, with semipermeable membrane as separator) and Device 3 (0.1 M SPAni + 4 M H_2SO_4, with porous cellulose acetate membrane as separator).

Conclusion

In conclusion, we have designed a novel type of supercapacitor (PAEESC), with electroactive polymers as additive in the electrolyte and semipermeable membrane as the separator. A PAEESC with SPAni as polymeric active electrolyte was fabricated. Owing to the pseudocapacitance provided by SPAni, the specific capacitance of the device was improved compared with the corresponding EDLSC. Furthermore, by using semipermeable dialysis membrane as the separator, the migration of SPAni between anode and cathode was blocked, thus the SDC process of the device was successfully suppressed. This research opens a new way to the AEESCs with both high capacitance and good energy retention. We believe that PAEESC is a promising type of supercapacitor, and its performance can be further improved in the future by designing advanced polymeric active electrolytes.

Acknowledgements

The authors thank the National Natural Science Foundation of China (21104041) for financial support.

Notes and references

College of Materials, Xiamen University, Xiamen, 361005, P. R. China. E-mail: baihua@xmu.edu.cn; lilei@xmu.edu.cn

†Electronic Supplementary Information (ESI) available: Characterization of SPAni, repeatability of the devices, AC impedance spectrum of Device 2, and other additional data. See DOI: 10.1039/b000000x/

1 Conway, B. E. *Kluwer Academic / Plenum Publishers: New York*, 1999.
2 M. S. Whittingham, *Proc. IEEE,* 2012, **100**, 1518−1534.
3 E. Frackowiak, F. Béguin, *Carbon*, 2001, **39**, 937−950.
4 L. L. Zhang, X. S. Zhao, *Chem. Soc. Rev.*, 2009, **38**, 2520−2531.
5 M. Inagaki, H. Konno, O. Tanaike, *J. Power Sources,* 2010, **195**, 7880−7903.
6 J. F. Mike, J. L. Lutkenhaus, *ACS Macro Lett*., 2013, **2**, 839−844.
7 C. D. Lokhande, D. P. Dubal, O. S. Joo, *Curr. Appl. Phys*., 2011, **11**, 255−270.
8 G. A. Snook, P. Kao, A. S. Best, *J. Power Sources,* 2011, **196**, 1−12.
9 S. Roldán, M. Granda, R. Menéndez, R. Santamaría, C. J. Blanco, *Phys. Chem. C,* 2011, **115**, 17606−17611.
10 S. Roldán, C. Blanco, M. Granda, R. Menéndez, R. Santamaría, *Angew. Chem. Int. Ed.,* 2011, **50**, 1699−1701.
11 S. T. Senthilkumar, R. K. Selvan, N. Ponpandian, J. S. Melo, *RSC Adv,* 2012, **2**, 8937−8940.
12 W. Chen, R. B. Rakhi, H. N. Alshareef, *Nanoscale*, 2013, **5**, 4134−4138.
13 L. H. Su, X. G. Zhang, C. H. Mi, B. Gao, Y. Liu, *Phys. Chem. Chem. Phys.*, 2009, **11**, 2195−2202.
14 Y. Tian, J. Yan, R. Xue, B. J. Yi, *Electrochem. Soc.*, 2011, **158**, A818−A821.
15 S. T. Senthilkumar, R. K. Selvan, Y. S. Lee, J. S. Melo, *J. Mater. Chem. A*, 2013, **1**, 1086−1095.
16 S. Roldán, M. Granda, R. Menéndez, R. Santamaría, C. Blanco, *Electrochim. Acta*, 2012, **83**, 241−246.
17 H. Yu, L. Fan, J. Wu, Y. Lin, M. Huang, J. Lin, Z. Lan, *RSC Adv.*, 2012, **2**, 6736−6740.
18 H. Yu, J. Wu, L. Fan, Y. Lin, S. Chen, Y. Chen, J. Wang, M. Huang, J. Lin, Z. Lan, Y. Huang, *Sci. China Chem.,* 2012, **55**, 1319−1324.
19 M. Tachibana, T. Ohishi, Y. Tsukada, A. Kitajima, H. Yamagishi, M. Murakami, *Electrochemistry*, 2011, **79**, 882−886.
20 L. B. Chen, H. Bai, Z. F. Huang, L. Li, *Energy Environ. Sci.*, DOI:10.1039/C4EE00002A 2014.
21 S. Ito, K. Murata, S. Teshima, R. Aizawa, Y. Asako, K. Takahashi, B. M. Hoffman, *Synth. Met.,* 1998, **96**, 161−163.
22 H. Bai, Y. X. Xu, L. Zhao, C. Li, G. Q. Shi, *Chem. Commun.,* 2009, 1667−1669.
23 W. S. Hummers, R. E. Offeman, *Chem. Soc.*, 1958, **80**, 1339-1339.
24 Y. Q. Chen, K. W. Chen, H. Bai, L. Li, *J. Mater. Chem.*, 2012, **22**, 17800−17804.
25 L. Zhang, G. Q. Shi, *J. Phys. Chem. C.*, 2011, **115**, 17206−17212.
26 K. X. Sheng, Y. X. Xu, C. Li, G. Q. Shi, *New Carbon Mater.,* 2011, **26**, 9−15.
27 A. J. Bard, L. R. Faulkner, Electrochemical methods: Fundamentals and applications. 2nd ed.; *John Wiley & Sons: New York*, 2001.
28 S. M. Paek, E. Yoo, I. Honma, *Nano Lett.,* 2008, **9**, 72−75.
29 J. Yue, Z. H. Wang, K. R. Cromack, A. J. Epstein, *J. Am. Chem. Soc.* 1991, **113**, 2665−2671.
30 E. T. Kang, K. G. Neoh, K. L. Tan, *Prog. Polym. Sci.*, 1998, **23**, 277−324.
31 S. Ban, J. Zhang, L. Zhang, K. Tsay, D. Song, X. Zou, *Electrochim. Acta*, 2013, **90**, 542−549.
32 B. E. Conway, W. G. Pell, T. C. Liu, *J. Power Sources*, 1997, **65**, 53−59.
33 B. W. Ricketts, C. Ton-That, *J. Power Sources*, 2000, **89**, 64-69.

TOC for

Electrochemical Supercapacitor with Polymeric Active Electrolyte

Libin Chen, Yanru Chen, Jifeng Wu, Jianwei Wang, Hua Bai*, and Lei Li*

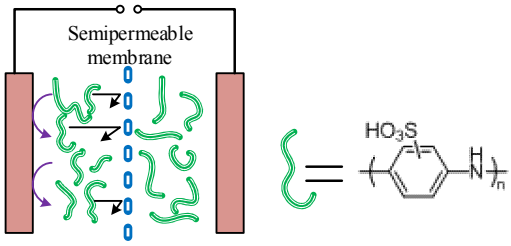

Supercapacitor with enhanced capacitance and energy retention was fabricated using sulfonated polyaniline as active electrolyte and semipermeable membrane as separator.